

Review

Review on the Selection of Health Indicator for Lithium Ion Batteries

Wenlu Zhou, Qiang Lu and Yanping Zheng * 

College of Automobile and Traffic Engineering, Nanjing Forestry University, Nanjing 210037, China; wenlulu1997_1@163.com (W.Z.); lqared@163.com (Q.L.)

* Correspondence: zhengyp@njfu.com.cn; Tel.: +86-138-5186-4173

Abstract: Scientifically and accurately predicting the state of health (SOH) and remaining useful life (RUL) of batteries is the key technology of automotive battery management systems. The selection of the health indicator (HI) that characterizes battery aging affects the accuracy of the prediction model construction, which in turn affects the accuracy of SOH and RUL estimation. Therefore, this paper analyzes the current status of HI selection for lithium-ion batteries by systematically reviewing the existing literature on the selection of HIs. According to the relationship between HI and battery aging, battery HI can be divided into two categories: direct HI and indirect HI. The capacity and internal resistance of the battery can directly represent the aging degree of the battery and are the direct HIs of the battery. Indirect HIs refer to characteristic parameters extracted from battery charge and discharge data that can characterize the degree of battery aging. This paper analyzes and summarizes the advantages and disadvantages of various HIs and indirect HIs commonly used in current research, providing useful support and reference for future researchers in selecting HIs to characterize battery aging. Finally, in view of the capacity regeneration phenomenon in the aging process of the battery, the selection direction of future HI is proposed.

Keywords: lithium-ion battery; battery aging; health indicator; direct HI; indirect HI



Citation: Zhou, W.; Lu, Q.; Zheng, Y. Review on the Selection of Health Indicator for Lithium Ion Batteries.

Machines **2022**, *10*, 512.

<https://doi.org/10.3390/machines10070512>

Academic Editor: Jie Liu

Received: 30 March 2022

Accepted: 22 June 2022

Published: 24 June 2022

Publisher's Note: MDPI stays neutral with regard to jurisdictional claims in published maps and institutional affiliations.



Copyright: © 2022 by the authors. Licensee MDPI, Basel, Switzerland. This article is an open access article distributed under the terms and conditions of the Creative Commons Attribution (CC BY) license (<https://creativecommons.org/licenses/by/4.0/>).

1. Introduction

With the rapid development of the automobile industry, the problems of energy consumption, environmental pollution and global warming are becoming more and more serious. It is crucial to develop and use energy-saving and environmentally friendly means of transportation. Vigorously developing new energy electric vehicles will contribute to building a clean, economical and efficient environmentally friendly society [1,2]. Power batteries are used as the power source of electric vehicles. Their performance directly affects the power, economy, safety and reliability of electric vehicles during driving [3]. With the continuous use of the battery, the battery will inevitably age or even fail. This will cause safety and reliability problems of the battery, and even cause the battery to spontaneously ignite and explode [4,5].

Both the SOH and RUL of the battery are important parameters to characterize the aging degree of the battery. The battery SOH is usually defined by the capacity ratio, that is, the ratio of the current actual battery capacity Q_{new} to the initial battery-rated capacity Q_0 , as shown in Formula (1). The battery RUL is the number of cycles of charge and discharge that the battery has undergone from the current capacity decay to the failure threshold [6]. The failure threshold of the battery is generally taken as 80% of the initial capacity [7]. According to the IEEE1188-1996 standard, when the battery capacity decays to the failure threshold, the battery capacity will decline rapidly according to the exponential decay trend. The battery performance at this time is no longer suitable for use as a power battery, and the battery should be replaced [8]. Therefore, the scientific and accurate prediction of battery SOH and RUL has become the key technology of automobile battery management

systems. In the research on battery SOH estimation and RUL prediction, the estimation method using the data-driven method and model method fusion has higher estimation accuracy [9,10]. Therefore, it is crucial to select the HI that can characterize the degree of battery aging. The quality of HI selection directly affects the accuracy of battery SOH and RUL prediction models, and further affects the prediction results.

$$SOH = \frac{Q_{new}}{Q_0} \times 100\% \tag{1}$$

At present, domestic and foreign researchers have achieved some important results in the selection of health indicators, as shown in Table 1. The correlation in Table 1 is the gray correlation value between the selected indirect health index and battery capacity decline. Compared with the relevant literature, this paper comprehensively and systematically analyzes the latest research results of the selection of HIs, summarizes the advantages and disadvantages of using different HIs to estimate the SOH and RUL of batteries, and summarizes the indirect HIs that are often selected in the current research. The purpose is to provide a reference for the selection of HIs for researchers who carry out this work in the future.

Table 1. Selection of HIs in the literature.

References	HI	HI Equations and Description	Correlation
[11]	Constant current charging time X_1	$X_1(k) = \{t(k) \min(t(k)), s.t. A(k) \leq 1.5 \text{ A}, k = 1, 2, \dots, n\}$ Among them, $t(k)$ represents the time when the constant current charging mode ends; $A(k)$ represents the measured current value; k is the current number of cycles; n is the sample size.	0.8763
	Average rate of change in voltage during constant current charging X_2	$X_2(k) = \frac{V(k)-v(k)}{t(k)}, k = 1, 2, \dots, n$ Among them, $v(k)$ and $V(k)$ represent the initial voltage value of the constant current charging process and the voltage value at the end of the constant current charging process, respectively; $t(k)$ is the charging time of the constant current charging process; k is the current number of cycles; n is the sample size.	0.6223
	Constant voltage charging time X_3	$X_3(k) = \{T(k) - t(k) \min(t(k)), s.t. V(k) \geq 4.2 \text{ V}, k = 1, 2, \dots, n\}$ Among them, $t(k)$ represents the moment when the measured voltage rises to 4.2 V, that is, the moment when the constant current charging ends; $T(k)$ represents the moment when the charging process ends; $V(k)$ represents the measured voltage value; k is the current cycle number; n is the sample size.	0.7104
	Average rate of change in current during constant voltage charging X_4	$X_4(k) = \frac{I(k)-i(k)}{t(k)}, k = 1, 2, \dots, n$ Among them, $i(k)$ and $I(k)$ represent the current value at the beginning and end of the constant voltage charging mode, respectively; $t(k)$ represents the time of constant voltage charging, k is the current number of cycles; n is the sample size.	0.9399
	The time for the surface temperature to rise to the highest during charging X_5	$X_5(k) = \{t(k) \max(T(k))\}, k = 1, 2, \dots, n$ Among them, $t(k)$ represents the time when the surface temperature rises to the highest during the charging process, $T(k)$ represents the measured surface temperature value, k is the current number of cycles, and n is the sample size.	0.9116

Table 1. Cont.

References	HI	HI Equations and Description	Correlation
[12]	the time of equal discharge voltage t_k	$t_k = T_{vmin} - t_{vmax}, k = 1, 2, \dots, n$ Among them, t_k represents the equal discharge voltage time of the k th cycle, T_{vmin} represents the time to reach the lower voltage value, and t_{vmax} represents the time to reach the upper voltage value.	0.8309
[13]	Current rate of change during constant current charging $I_{CCCR_{CV}}$	$I_{k_CCCR_{CV}} = B_k, k = 1, 2, \dots, n$ Among them, B_k is the charging current change rate of the k th cycle, and n is the sample size. k is the current number of cycles, and n is the sample size.	0.9776
[14,15]	The peak intensity of IC curve (IC_peak)	IC_peak is the normalized intensity of the IC peak	high correlation
[16]	The peak area of IC curve (IC_area)	$IC_area = \int_{U_{low}}^{U_{up}} w dV = \sum_{k=1}^m w_k, k = 1, 2, \dots, n$ where w is the value of dQ/dV ; w_k is the discrete values of w corresponding to different voltage interval, k is the current number of cycles, and n is the sample size.	high correlation
[17]	Average charge voltage rise (ACVR)	$ACVR_k = \frac{\sum_{j=1}^{100} V_T - V_j }{100}, k = 1, 2, \dots, n$ Among them, V_j is the voltage within the charging time from 1000 to 1500 s, V_T is the cut-off voltage, k is the current cycle number, and n is the sample size.	0.9940

2. Lithium-Ion Battery Health Indicator

The battery HI is generally obtained by processing the battery charge and discharge data through technologies such as signal processing and artificial intelligence. In the selection of lithium-ion battery HI, it is usually divided into two categories: direct HI and indirect HI [18], as shown in Figure 1. The most obvious characteristic of battery aging is the reduction in battery usable capacity and the increase in internal resistance. Therefore, the battery capacity and internal resistance are the direct HI that characterize the aging degree of the battery. Indirect battery HI refers to the extraction of indirect characteristic parameters that have strong correlation with battery aging from battery charge and discharge data, in addition to capacity and internal resistance.

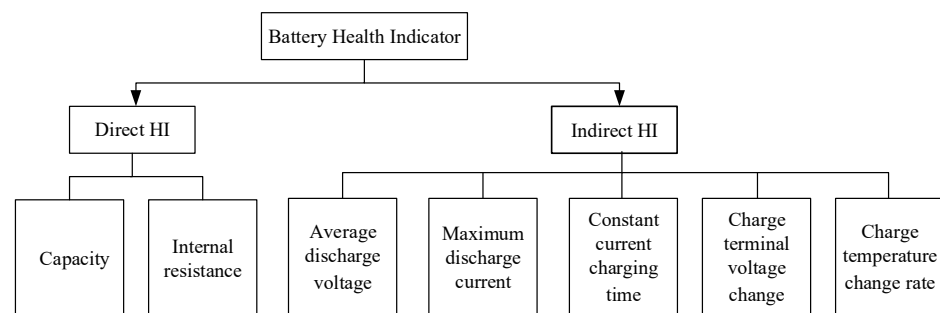


Figure 1. Classification of battery health indicators.

2.1. Direct Health Indicator

2.1.1. Battery Capacity

It can be seen from Formula (1) that the attenuation of the actual capacity of the battery will cause the overall SOH to show a declining trend, and the battery will age. Therefore, the battery capacity can be used as a direct HI for evaluating the degree of battery aging. The actual capacity of the battery is the maximum power that the battery can release when fully discharged under the specified discharge conditions. Its value can be calculated by integrating the current over time. Due to the limitation of test conditions, many researchers have studied battery RUL based on battery test data published by the Center for Advanced Lifecycle Engineering at the University of Maryland (CALCE, College Park, MD, USA) and National Aeronautics and Space Administration (NASA, San Francisco, CA, USA) [19]. Figure 2 shows the capacity data of B5, B6, B7, and B18 batteries disclosed by NASA. The capacity decay curve formed by arranging the battery capacity data according to the number of cycles conforms to the time series and has obvious nonlinear characteristics. The support vector regression (SVR) method can better solve nonlinear problems [20,21]. Therefore, some literatures use the battery capacity in the NASA and CALCE battery data sets as the HI for evaluating battery aging, and use SVR to predict the battery RUL. However, SVR has the problems of difficult parameter selection and low prediction accuracy. Therefore, intelligent algorithms such as gray wolf optimization and ant lion optimization are often used to optimize the SVR kernel parameters, thereby improving the accuracy of battery life prediction [22,23].

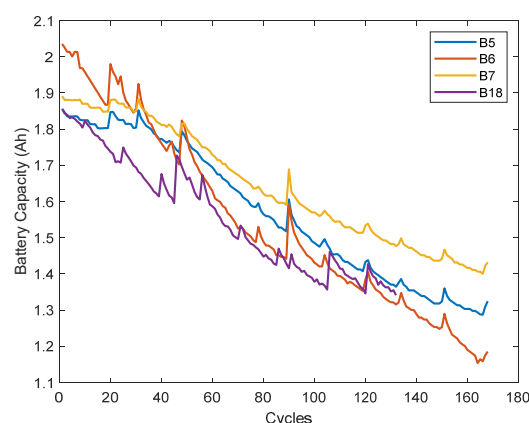


Figure 2. Battery Capacity Decay Curve.

Li-ion battery systems typically exhibit nonlinear and non-Gaussian behavior. Compared to the Kalman filter (KF) algorithm [24], which is applied to Gaussian noise and linear model problems, the particle filter (PF) algorithm can handle arbitrary nonlinear models. Therefore, the particle filter algorithm has a higher prediction accuracy and stability for battery life [25,26]. Therefore, some researchers established a battery aging model based on the capacity decay curve obtained from the public data set, and combined the PF algorithm to predict the battery life. For example, reference [27] takes the battery capacity as the health indicator, and achieves the RUL prediction of lithium-ion batteries based on the double exponential model and the PF algorithm. Reference [28] establishes a new capacity degradation model based on the battery capacity degradation curve, and uses the PF algorithm to improve the accuracy of the remaining life prediction of lithium-ion batteries. However, the PF algorithm suffers from particle degradation and particle barrenness. The resampling strategy can solve this problem to a certain extent, but it leads to the loss of particle diversity [29,30]. Another strategy is to choose a reasonable proposal density distribution. The unscented particle filter (UPF) algorithm uses the unscented Kalman filter (UKF) algorithm as the proposed density distribution, which improves the particle degradation problem and improves the prediction accuracy [31]. For example, the reference [32] introduces the

UKF algorithm and the linear optimization combined resampling algorithm into the basic PF algorithm. Therefore, a fusion UPF algorithm is proposed to predict battery life, and the effectiveness of the method is experimentally verified. To further improve the accuracy of RUL prediction, the UPF algorithm is used to dynamically estimate drift parameters and system states. Reference [33] uses the UPF algorithm to dynamically estimate the drift parameters and system state to further improve the RUL prediction accuracy. Reference [34] used the double exponential empirical model fitting method to obtain the initial values of the model parameters based on the capacity decay curve. Finally, the random disturbance unscented particle filter algorithm is used to update the model parameters to predict the remaining life of lithium-ion batteries and give the probability distribution of the prediction results. The aging degree of lithium-ion batteries can be accurately expressed by capacity. However, the battery capacity is usually obtained by calculating the complete charging and discharging process by the ampere–hour integration method, which is time-consuming and has accumulated errors in the ampere–hour integration method. Additionally, in practical applications, lithium-ion batteries are generally not in a fully charged and discharged working state. Therefore, the battery capacity is difficult to obtain online.

2.1.2. Battery Internal Resistance

In addition, with the continuous cycling of the battery, the internal resistance of the battery will gradually increase with the increase of the number of charge and discharge cycles. The increase in the internal resistance of lithium-ion batteries can cause failure problems such as a decrease in discharge voltage and power, a decrease in energy density, and an increase in battery temperature [35]. Therefore, the internal resistance of lithium-ion batteries can also be used as a direct HI to characterize the aging degree of the battery. In the field of electric vehicle power batteries, it is generally considered that the failure threshold of the battery is when the internal resistance of the battery increases twice [36]. The internal resistance of the battery is usually obtained by electrochemical impedance spectroscopy (EIS) analysis using the equivalent circuit model, as shown in Figure 3 [37,38].

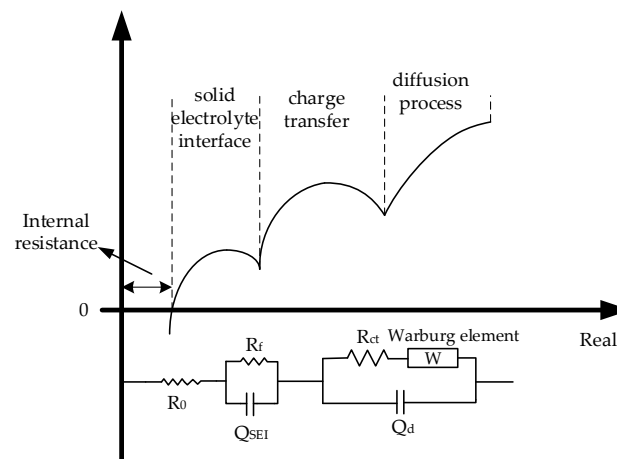


Figure 3. Equivalent circuit model and its correspondence with different regions of EIS.

As shown in Figure 3, the intersection of the EIS curve and the horizontal axis is described by the ohmic resistance (R_0). The high-frequency arc is related to the impedance of the battery EIS film, described by the film resistance (R_f) and the interfacial layer capacitance (Q_{SEI}) caused by the dispersion effect. The intermediate frequency arc represents the reaction impedance of the solid–liquid electrode interface, which is described by the charge transfer resistance (R_{ct}) of the interface reaction and the electric double layer capacitance (Q_d) caused by the dispersion effect [37]. The larger the arc of the intermediate frequency, the greater of the load transfer resistance during the aging process of the battery. The straight line approximated by the low-frequency band is related to the diffusion process

of lithium ions in the electrode solid phase material, which is described by the Warburg element of the diffusion impedance of lithium ions in the solid phase particles [39]. Therefore, using the equivalent circuit model to analyze the EIS at different aging stages can obtain the evolution law of the impedance components corresponding to different processes with the aging of the battery. In turn, the current battery SOH and RUL predictions are achieved. In the early RUL prediction of lithium-ion batteries, only using the R_0 as HI has a large error [40]. Reference [41] takes battery capacity, R_0 and R_{ct} as HI. Additionally, the extended Kalman filter and particle filter algorithms are used to predict the battery RUL, respectively. Among them, R_{ct} characterizes the difficulty of the electrode interface reaction during battery aging. Therefore, using R_{ct} as battery HI provides a new idea for battery SOH and RUL prediction. The resistance of the battery R_{ct} increases significantly with the aging of the battery, which exhibits a first-order polynomial variation law. Therefore, the battery-aging empirical model can be selected according to the principle of the smallest fitting error of its decay change law. Additionally, use the particle filter algorithm to predict the battery RUL, so as to achieve the efficient management and maintenance of the battery [38]. However, the resistance value and growth rate of R_{ct} are also affected by the temperature and the state of charge (SOC) of the battery [42]. Therefore, reference [43] studies the R_{ct} at different temperatures and SOC as the battery HI to estimate the battery SOH. The research results show that the uncertainty of the R_{ct} obtained by fitting the EIS at high SOC and high temperature is high, which makes the SOH estimation have a large error. The R_{ct} obtained by fitting the EIS at 50% SOC and 298 K has the highest estimation accuracy for the battery SOH. It can be seen from the above content that the change in the internal resistance of the battery can characterize the aging state of the battery. However, in the actual application process, it is a very complicated and time-consuming thing to measure the internal resistance of the battery by EIS. Additionally, this process requires professional testers and a harsh test environment. Therefore, it is difficult to carry out engineering application.

Both battery capacity and internal resistance are important indicators to characterize battery SOH and RUL. However, using the capacity or internal resistance as the direct HI of the battery needs a many laboratory or offline tests. It not only requires sophisticated instruments and equipment, but also excludes external environmental interference factors, so online acquisition and real-time prediction cannot be achieved. Therefore, how to extract indirect HI from monitorable state parameters has become a hot issue for researchers.

2.2. Indirect Health Indicator

The indirect HI of a battery refers to a characteristic parameter extracted from the battery charge and discharge data that can characterize the degree of battery aging, except for capacity and internal resistance, which has a strong correlation with the battery aging characteristics. Constructing a simple and easy-to-measure indirect HI can solve the problem that direct HI is difficult to obtain online. It can also characterize battery aging well and be used for battery SOH and RUL prediction [44,45]. The flow of battery SOH and RUL prediction based on indirect HI is shown in Figure 4 [17,46].

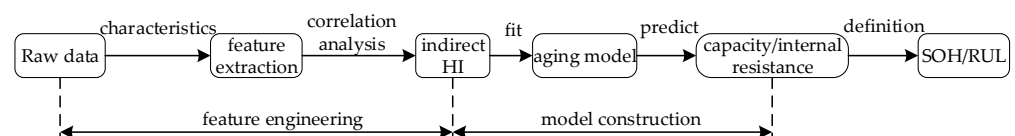


Figure 4. Flowchart for Predicting Battery SOH and RUL Based on Indirect HI.

As can be seen from Figure 4, the prediction process is mainly divided into two stages: feature engineering and model construction. Feature engineering mainly analyzes the original data and analyzes the external data during the charging and discharging stage of the battery. The characteristic parameters that can characterize the aging degree of the battery are extracted from it. After correlation analysis is performed on the extracted

parameters, the feature parameters with high correlation are used as the indirect HI of the battery. Model construction is to build a battery aging model based on the extracted indirect HI. As the battery ages, external data such as battery voltage, current, and temperature change, as shown in Figure 5. Therefore, researchers usually extract the battery indirect HI from the voltage, current and temperature data that are easily monitored online to characterize the battery aging state.

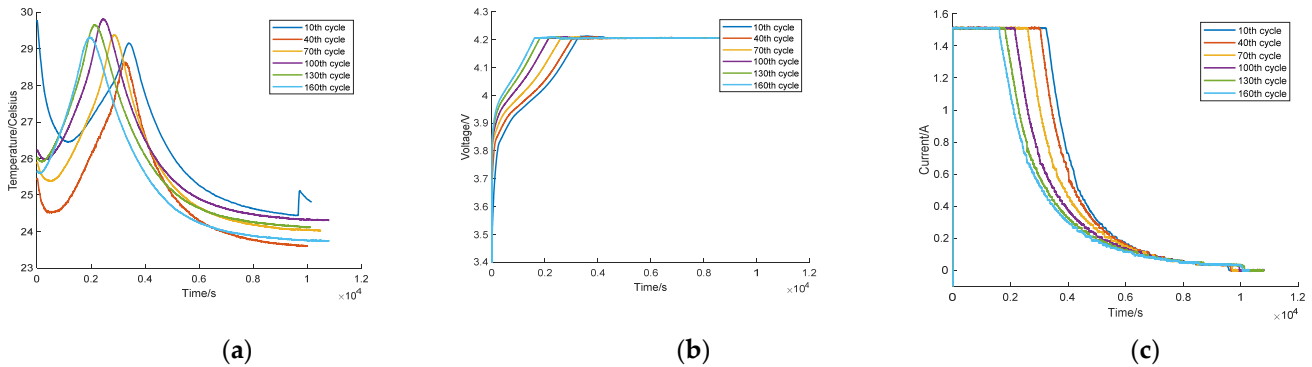


Figure 5. Battery-charging process with different cycles: (a) battery temperature change curve; (b) battery voltage change curve; (c) battery current change curve.

2.2.1. Indirect HI Based on Discharge Process

During the discharge process of a battery, it takes a period of time for its voltage to drop from a relatively high voltage to a lower voltage [47]. This time will decrease as the number of battery charge–discharge cycles increases. Therefore, taking the discharge time of equal voltage drop as the indirect HI of the battery can be used to estimate the aging state of the battery [48]. With the increase in the number of charge–discharge cycles of the battery, the rate of decrease in the discharge voltage gradually becomes faster. Therefore, using the voltage difference change in the same time interval as the battery indirect HI can also characterize the aging state of the battery [49]. In the battery cycle charge and discharge test, when the discharge current is the same, the duration of the discharge process directly affects the battery discharge capacity. Therefore, taking the duration of the discharge process as the indirect HI can characterize the aging state of the battery [50]. Other studies have found a strong linear correlation between battery capacity decay and the rate of change in battery temperature. Therefore, the temperature change rate as the indirect HI can also well characterize the aging degree of the battery, and the prediction accuracy of the SOH and RUL of the battery is high [51]. In the external data based on the battery discharge stage, researchers also often extract the discharge voltage sample entropy, average voltage and average current as the battery indirect HI. Reference [44] extracted the mean value of voltage fluctuation over a period of time from the battery discharge curve as an indirect HI for battery RUL prediction.

Because the battery initial data are complex and non-linear, it is necessary to preprocess the data and the extracted feature parameters. In view of the influence of measurement noise in the battery data acquisition process, reference [52] uses wavelet transform to preprocess the data to remove the noise in the data acquisition process. At the same time, there is a local capacity regeneration phenomenon in the battery aging data. The data can be smoothed using empirical mode decomposition techniques. Reference [53] uses the battery capacity and the discharge voltage difference at equal time intervals as the battery indirect HI, and uses the phase space reconstruction method to reconstruct the time series of the extracted HI. Additionally, the ensemble empirical mode decomposition method is used to preprocess the reconstructed time series data of the two HIs to avoid the influence of data noise. Finally, combined with genetic algorithm and support vector machine, the battery RUL is predicted. In addition to the above methods for smoothing the initial data, methods such as moving average and Gaussian filtering are often used [54,55].

2.2.2. Indirect HI Based on Charging Process

The above-mentioned indirect HI extracted based on the battery discharge stage and changed with the increase in the number of cycles of charging and discharging can characterize the aging state of the battery. Additionally, indirect HI can achieve online monitoring and easy direct measurement. However, the indirect HI extracted based on the battery discharge stage is often only suitable for fixed constant current discharge conditions. However, in practical applications, it is difficult for lithium-ion batteries to maintain a constant current state for continuous discharge. Compared with the complex and changeable discharge process, the charging process of the battery is often in the constant current-constant voltage mode, and the working conditions are relatively stable and less affected by external factors. Additionally, in practical applications, the battery is often used after it is fully charged, so the indirect HI extracted based on the battery charging stage will be more in line with practical applications.

As the battery is continuously charged and discharged, the polarization degree of the battery deepens, and the duration of constant current charging decreases. The constant current charging duration of the battery directly affects the amount of power charged into the battery, and can also characterize the degree of polarization of the battery. Therefore, the constant current charging duration can be used as an indirect HI to characterize the aging degree of the battery [56]. As the number of battery cycles increases, the battery terminal voltage also has a significant difference. Therefore, reference [57] regards the terminal voltage difference during the charging process of different cycles as the indirect HI, and achieves the battery RUL prediction based on the combination of a feedforward neural network and importance sampling. Some studies have also shown that the charging voltage curve of the battery has a good consistency with the battery capacity decline. Therefore, the charging voltage curve can be used to characterize the aging degree of the current battery. However, in the actual use of the battery, it is often difficult to obtain a complete charging voltage curve. Therefore, some researchers use the traversal optimization method to find the optimal voltage segment, and extract the equal voltage rise time of the optimal voltage segment as the indirect HI. Based on this, a battery aging model is established [58]. Some researchers also use the particle swarm optimization algorithm to obtain the optimal voltage or current variation range during the battery charging phase. It avoids that the voltage and current of the battery are in a fully charged and discharged state, which is more in line with the actual working range of the battery [59–61].

In addition to extracting indirect HI from data external to the battery, one can also start with mathematical geometry. Reference [62] selects the duration of the constant voltage charging mode, the duration of the constant current charging mode and the slope at the turning point of the constant current charging mode as indirect HI. The grey correlation degree method was used to analyze the correlation degree between the selected HI and the battery aging state. Reference [63] uses the arc length, normal and curvature of the battery during the constant current charging phase to characterize the state of health of the battery. Additionally, the battery aging model based on mathematical geometry HI is established to predict the battery SOH through the neural network algorithm.

Theoretically, the change in the voltage of the battery during operation can reflect its internal electrochemical properties. However, the information observed in the normal charge-discharge curve is very limited, and the electrochemical changes in the positive and negative electrodes of the battery cannot be accurately analyzed. Therefore, some researchers conduct analysis based on the incremental capacity (IC) curve, and extract health indicators that can reflect battery aging from the IC curve to predict battery life [64,65]. The battery capacity increment is obtained by calculating the change in capacity due to a unit voltage change (dQ/dV) in a voltage-capacity (V-Q) curve for constant current charging. That is, the capacity increment curve is derived from the V-Q curve, but in practice the numerical difference ($\Delta Q/\Delta V$) is usually used instead of dQ/dV [66]. In the case of constant current charge and discharge, the IC curve is related to the derivative (dV/dt) of the voltage-time curve, as shown in Equation (2). Therefore, the capacity increment curve can convert the

voltage plateau that is difficult to observe and analyze with slow voltage changes during the charging process of the battery into a peak value on the capacity increment curve that is easy to observe and analyze [67,68]. The battery IC curve is shown in Figure 6. It can be seen from (a) and (b) of Figure 6 that the multiple health indicators can be extracted from the IC peaks (peak A, peak B), including peak height, peak position, peak area, peak width, and the left and right slope of the peak. Through the change in these parameters, the aging mechanism of the battery can be analyzed to predict the remaining service life of the battery. In order to improve the accuracy of battery SOH estimation, reference [69] extracts HIs from different peak intervals of the battery IC curve, and selects the peak interval with high correlation with battery SOH for battery SOH estimation. The influence of the peak interval on the SOH estimation is verified with the data of the 5th, 6th, 7th and 18th batteries provided by NASA, and the selected peak interval can meet the high-precision requirements of the battery SOH estimation. Reference [70] uses the battery static charging curve to extract the peak position and peak valley position of the IC curve as HIs to predict the battery life. The research results show that extracting the HIs on the IC curve can not only meet the estimation accuracy, but also reduce the computational complexity. The reference [47] extracts multiple HIs based on the IC curve, and simplifies the HIs from two aspects of data quality and practical application, and establishes a battery aging model to predict battery life. The reference [71] selects the fixed voltage interval on the left and right sides of the peak value of the IC curve to obtain the discharge area capacity under the fixed voltage interval, thereby establishing a linear function of the area capacity and SOH. The NASA battery data set is used for verification, and the results show that the estimation error of SOH is less than 2.5%. The reference [72] extracts the peak of the IC curve and the area under the peak as health indicators, and proposes a new method for RUL prediction of lithium-ion batteries that fuses incremental capacity analysis and Gaussian regression process.

$$IC = \frac{dQ}{dV} \approx \frac{\Delta Q}{\Delta V} = \frac{I \times t}{\Delta V} = \frac{I}{\Delta V / \Delta t} \quad (2)$$

Table 2. Battery Indirect HI selection.

discharge process	total voltage at the beginning of discharge, total voltage at the end of discharge, time interval of equal voltage drop, voltage difference at the same time interval, sample entropy of discharge voltage, rate of temperature change during discharge, battery capacity increment, depth of discharge, maximum discharge current, average voltage, average current, maximum feedback current, capacity increment curve in discharge stage.
charging process	terminal voltage change, time of constant current charging process, time of constant voltage charging process, total time of charging stage, maximum slope of charging voltage curve, maximum slope of charging current curve, slope at the turning point of constant current charging mode, temperature change in charging stage, equal voltage rise charging time, equal time interval charging voltage rise, equal time interval charging current drop, average voltage decay, battery capacity increment, arc length, normal and curvature changes in the constant current charging phase.

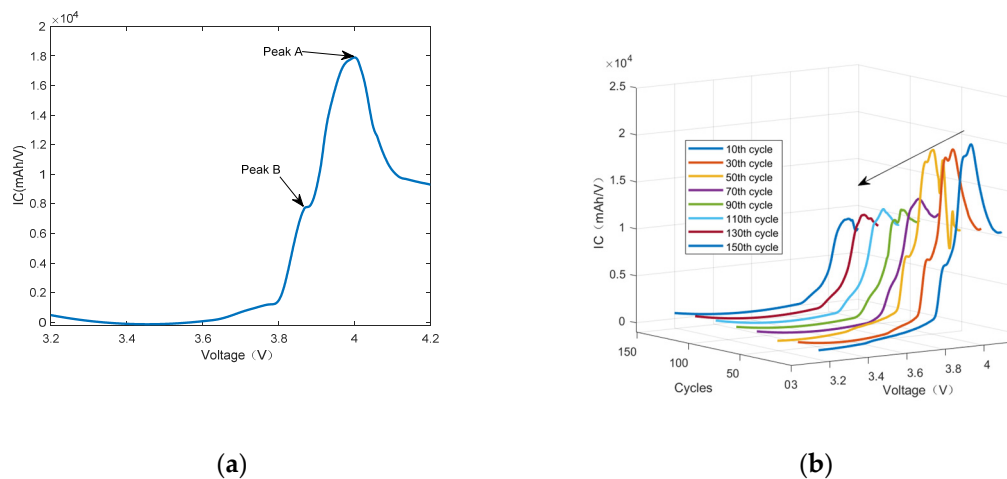


Figure 6. Battery capacity increment curve: (a) IC curve of a single cycle; (b) IC curve of multiple cycles. A summary of the indirect HIs that can be selected based on the battery charge and discharge stages is shown in Table 2.

In the formula, IC represents the capacity increment value of the battery; Q represents the battery capacity during charging; V represents the terminal voltage of the battery; I represents the charging current of the battery; t represents the charging time of the battery.

2.2.3. Fusion of HIs

Compared with the battery aging model based on a single indicator, the multi-indicator fusion battery aging model has higher prediction accuracy. Additionally, as the number of battery HI increases, the prediction accuracy gradually improves, in order to make up for the lack of a single indicator to establish a battery aging model. Reference [73] extracted the charging current difference and voltage difference at different time intervals as indirect HI from the relatively stable charging process, and established a linear regression model of battery aging. The battery life decline is affected by a variety of factors. Temperature is also a key factor affecting battery cycle life. Therefore, the reference [74] extracts the constant current charging time, the time change in the constant pressure difference and the temperature change during the constant current charging stage as the indirect HI. The multi-indicator fusion of the extracted HIs was carried out using the grey relational analysis method and the entropy weight method. Finally, based on the indirect HI obtained by the fusion of multiple indicators, a battery aging model is established to predict the battery RUL.

When predicting battery SOH and RUL based on multi-indicator fusion, the trend in HI changes is different for different batteries. Therefore, it is difficult to directly judge the degree of correlation between it and battery aging. In order to select a HI that is highly correlated with battery aging, researchers often use methods such as Pearson, Spearman correlation coefficient and grey correlation analysis to calculate the degree of correlation between the extracted indirect HI and battery capacity decline [75,76].

The grey relational degree analysis quantitatively analyzes the similarity and difference between the reference sequence and the surrogate sequence from the similarity degree of the geometric curves of the two variable sequences [77]. The Pearson correlation coefficient measures the degree of association between two variable series from the perspective of the linear correlation of the two variable series. The Pearson correlation coefficient can well describe whether there is a linear relationship between two variable series, but it is greatly affected by outliers [78]. Compared with the Pearson correlation coefficient, the Spearman correlation coefficient has a better ability to deal with abnormal data. The scope of application of the two is also different. When the selected variable is a continuous function and obeys a normal distribution, using the Pearson correlation coefficient has a better effect. If any of the above conditions are not met, the Spearman correlation coefficient

is more efficient [54,79]. In addition, some researchers employ Box–Cox variation to improve the correlation between feature quantities and estimators [80,81]. By performing Box–Cox changes on the historical data of lithium-ion batteries, the nonlinear capacity decay trajectory can be linearized, which can greatly improve the prediction accuracy of the linear model and effectively reduce the difficulty of battery RUL prediction.

There must be overlapping information between HIs that are highly correlated with battery aging. At this time, principal component analysis (PCA) is often used to reduce dimensionality and remove redundancy for multiple HIs. PCA can reconstitute the original higher number of variables into several fewer interrelated comprehensive variables while maintaining the original information as much as possible [82,83]. Reference [84] used the grey correlation degree to perform correlation analysis on the extracted 10 potential HIs, and used PCA to fuse the data. The processed data are used as the input to the aging model for RUL prediction of the battery. The research results show that the method has high prediction accuracy. Compared with the PCA method, the mutually independent HI extracted based on the kernel principal components analysis (KPCA) method can more significantly reflect the battery performance degradation. It can reduce the influence of noise while reducing parameter redundancy. Reference [85] uses KPCA to extract characteristic parameters and fuse multiple indicators for the measurable discharge current and voltage of the battery. Then, they use the Spearman correlation coefficient to select the characteristic parameter with high correlation with battery aging as HI. Finally, the battery life is predicted based on the adaptive neural network fuzzy inference system. Studies have shown that the HI extracted by this method is highly correlated with battery aging. Fusion of multiple indirect HIs without overlapping information can greatly improve the accuracy of battery life prediction. It can be seen that the indirect HI extracted from the external data of the battery can well characterize the aging degree of the battery. At the same time, it also avoids the defect that direct HI cannot be obtained online and predicted in time [86,87], considering that the external data obtained in the battery discharge stage is greatly affected by external factors. Therefore, the indirect HI extracted based on the battery-charging stage is more suitable for practical applications. Moreover, the battery aging model established by multi-indicator fusion of multiple indirect HIs extracted during the charging phase is more accurate than the aging model established based on a single indicator.

3. Summary

In this paper, a review is carried out on the relevant work and research results of the selection of health indicators of lithium-ion batteries. The advantages and disadvantages of direct HI and indirect HI to characterize the aging degree of batteries are summarized. The conclusions and prospects are as follows:

(1) When using the battery direct HI to estimate the battery SOH and predict the RUL, the step of extracting the indirect HI through feature engineering can be omitted, and the battery SOH and RUL have high estimation accuracy. However, online monitoring and real-time acquisition of battery capacity cannot be achieved, and it is very complicated and time-consuming to use electrochemical impedance spectroscopy to measure battery internal resistance. Therefore, SOH and RUL estimation based on direct health indicators are difficult to apply in practical engineering.

(2) Constructing simple and easy-to-measure indirect HIs from battery external data can solve the problem that a direct HI is difficult to obtain online, and can also well characterize battery aging characteristics. The external data of the battery during the discharge phase are not objective enough due to the different individual usage habits and usage environments. In the charging phase of the battery, the car is in a stopped state; the battery does not provide energy to the outside world and is less affected by external factors. Therefore, the indirect HI based on battery charging stage data extraction is more accurate and stable for battery SOH and RUL prediction.

(3) After the correlation analysis and multi-indicators fusion of multiple indirect HIs of the battery, the established battery aging model has higher prediction accuracy than the battery aging model established based on a single HI.

The advantages and disadvantages of various health indicators are summarized in Table 3.

Table 3. Comparison of advantages and disadvantages of various HIs.

HI	Classification	Advantage	Disadvantage
Direct HI	Battery Capacity	Directly characterize battery aging with high accuracy for battery SOH estimation and RUL prediction	It is impossible to realize online monitoring and real-time acquisition; it is calculated by the \int -integral method, which is time-consuming and has accumulated errors
	Battery Internal Resistance	Strong correlation with battery aging	Measuring battery internal resistance with EISEIS is complex and time-consuming
Indirect HI	HIs Extracted Based on The Discharge Process	The aging state of the battery can be monitored online	Affected by external factors, the collected data are not objective enough
	HIs Extracted Based on The Charging Process	Less affected by external factors, the collected data are relatively accurate	Unable to monitor battery aging status while the car is in motion
Fusion of multiple HIs		Considering multiple factors that affect the aging of battery performance, fully including the aging information of the battery	The amount of calculation increases and there is redundant information between multiple health indicators, which requires preprocessing

4. Future Development

The side reactions between the electrolyte and the electrodes during the charge and discharge of ion batteries can lead to the deterioration of the battery chemistry. When the battery is in a static state, the electrochemical performance is recovered to a certain extent, and the battery has a local capacity regeneration phenomenon. The HI in the actual operating state of the lithium-ion battery not only contains the information on the overall decay trend in the battery. It also includes local regeneration components and noise fluctuation components caused by battery standing. It exhibits nonlinear and non-stationary characteristics. Therefore, in the future, suitable preprocessing methods should be studied to deal with the inaccurate prediction of battery RUL due to the instability of HI, and health indicators that can reflect the phenomenon of battery capacity regeneration should be selected.

Author Contributions: All authors contributed to the publication of this article. All authors have carefully studied the relevant literature on the selection of health indicators for Li-ion batteries. W.Z. is mainly responsible for the overall idea of arranging the dissertation, as well as the writing and subsequent revision of the dissertation. Q.L. is mainly responsible for arranging the materials required for the thesis and cooperating with W.Z. in the writing. Y.Z. provided technical guidance during the writing and revision of the dissertation. All authors have read and agreed to the published version of the manuscript.

Funding: This research was funded by Jiangsu Provincial Key R&D Program: Optimization and Integration Technology of Electric Vehicle Battery and Energy Management System, Grant No. BE2017008.

Data Availability Statement: Not applicable.

Conflicts of Interest: The authors declare no conflict of interest.

References

1. Tucki, K.; Orynych, O.; Świć, A.; Mitoraj-Wojtanek, M. The Development of Electromobility in Poland and EU States as a Tool for Management of CO₂ Emissions. *Energies* **2019**, *12*, 2942. [CrossRef]
2. Gomes, E. Sustainable Population Growth in Low-Density Areas in a New Technological Era: Prospective Thinking on How to Support Planning Policies Using Complex Spatial Models. *Land* **2020**, *9*, 221. [CrossRef]
3. Zang, P.; Dong, W.; Ma, B. Overview of research on echelon utilization of electric vehicle power batteries. In Proceedings of the 3rd Smart Grid Conference-Smart Power Consumption, Beijing, China, 27–30 October 2019; pp. 484–486.
4. Jiang, J.; Gao, Y.; Zhang, C. On-line diagnosis method of electric vehicle lithium-ion power battery health status. *Chin. J. Mech. Eng.* **2019**, *55*, 60–72.
5. Yao, J.; Li, Z.; Wang, M. Automobile active tilt control based on active suspension. *Adv. Mech. Eng.* **2018**, *10*, 168781401880145. [CrossRef]
6. Jiao, Z.; Fan, X.; Zhang, X. State Tracking and Remaining Service Life Prediction Method of Li-ion Battery Based on Improved Particle Filter Algorithm. *Chin. J. Electrotech. Technol.* **2020**, *35*, 3979–3993.
7. Lin, C.P.; Cabrera, J.; Yang, F.; Ling, M.H.; Tsui, K.L.; Bae, S.J. Battery state of health modeling and remaining useful life prediction through time series model. *Appl. Energy* **2020**, *275*, 115338. [CrossRef]
8. Wu, L.; Fu, X.; Guan, Y. Review of the Remaining Useful Life Prognostics of Vehicle Lithium-Ion Batteries Using Data-Driven Methodologies. *Appl. Sci.* **2016**, *6*, 166. [CrossRef]
9. Noura, N.; Boulon, L.; Jemeï, S. A Review of Battery State of Health Estimation Methods: Hybrid Electric Vehicle Challenges. *World Electr. Veh. J.* **2020**, *11*, 66. [CrossRef]
10. Xiong, R.; Li, L.; Tian, J. Towards a smarter battery management system: A critical review on battery state of health monitoring methods. *J. Power Sources* **2018**, *405*, 18–29. [CrossRef]
11. Song, D. Lithium Battery State of Health Assessment Based on Surface Temperature Characteristics. Master's Thesis, Xidian University, Xi'an, China, 2021.
12. Li, W.; Jiao, Z.; Du, L.; Fan, W.; Zhu, Y. An indirect RUL prognosis for lithium-ion battery under vibration stress using Elman neural network. *Int. J. Hydrogen Energy* **2019**, *44*, 12270–12276. [CrossRef]
13. Wang, R. Prediction of the Remaining Life of Lithium Batteries Based on New Health Indicators. Master's Thesis, Xidian University, Xi'an, China, 2020.
14. Tian, J.; Xiong, R.; Yu, Q. Fractional order model based incremental capacity analysis for degradation state recognition of lithium-ion batteries. *IEEE Trans. Ind. Electron.* **2019**, *66*, 1576–1584. [CrossRef]
15. Zhang, Y.C.; Briat, O.; Delétage, J.Y.; Martin, C.; Chadourne, N.; Vinassa, J.M. Efficient state of health estimation of Li-ion battery under several ageing types for aeronautic applications. *Microelectron. Reliab.* **2018**, *88*, 1231–1235. [CrossRef]
16. Tang, J.; Liu, Q.; Liu, S.; Xie, X.; Zhou, J.; Li, Z. A health monitoring method based on multiple indicators to eliminate influences of estimation dispersion for lithium-ion batteries. *IEEE Access* **2019**, *7*, 122302–122314. [CrossRef]
17. Zhang, W.; Wang, W. Capacity estimation of lithium-ion batteries based on new health indicators. *Electron. Meas. Technol.* **2020**, *43*, 10–15. [CrossRef]
18. Khumprom, P.; Yodo, N. A Data-Driven Predictive Prognostic Model for Lithium-ion Batteries based on a Deep Learning Algorithm. *Energies* **2019**, *12*, 660. [CrossRef]
19. Nieto, P.G.; García-Gonzalo, E.; Lasheras, F.S.; de Cos Juez, F.J. Hybrid PSO-SVM-based method for forecasting of the remaining useful life for aircraft engines and evaluation of its reliability. *Reliab. Eng. Syst. Saf.* **2015**, *138*, 219–231. [CrossRef]
20. Gao, L.; Xu, F.; Li, H. Recognition method of sheet surface defects based on deep learning features and nonlinear support vector machine. *Chin. J. For. Eng.* **2019**, *4*, 99–106.
21. Sun, S. A new stress field intensity model and its application in component high cycle fatigue research. *PLoS ONE* **2020**, *15*, e0235323. [CrossRef]
22. Yang, Z.; Wang, Y.; Kong, C. Prediction of the remaining service life of lithium batteries based on GWO-SVR. *J/OL J. Power Supply*. 2021. Available online: <http://kns.cnki.net/kcms/detail/12.1420.TM.20210520.1300.002.html>.
23. Wang, Y.; Ni, Y.; Zheng, Y. Prediction of the remaining service life of lithium-ion batteries based on ALO-SVR. *Chin. J. Electr. Eng.* **2021**, *41*, 1445–1457.
24. Duong, P.; Raghavan, N. Heuristic Kalman optimized particle filter for remaining useful life prediction of lithium-ion battery. *Microelectron. Reliab.* **2018**, *81*, 232–243. [CrossRef]
25. Guha, A.; Patra, A. State of Health Estimation of Lithium-Ion Batteries Using Capacity Fade and Internal Resistance Growth Models. *IEEE Trans. Transp. Electrif.* **2018**, *4*, 135–146. [CrossRef]
26. Pan, C.; Huang, A.; He, Z. Prediction of remaining useful life for lithium-ion battery based on particle filter with residual resampling. *Energy Sci. Eng.* **2021**, *9*, 1115–1133. [CrossRef]
27. Zhang, L.; Mu, Z.; Sun, C. Remaining Useful Life Prediction for Lithium-Ion Batteries Based on Exponential Model and Particle Filter. *IEEE Access* **2018**, *6*, 17729–17740. [CrossRef]
28. Li, Y.; Lin, S.; Yuan, X. Research on RUL Prediction of Lithium Batteries Based on New Capacity Degradation Model. *Comput. Simul.* **2020**, *37*, 120–124. [CrossRef]

29. Jouin, M.; Gouriveau, R.; Hissel, D. Particle filter-based prognostics: Review, discussion and perspectives. *Mech. Syst. Signal Process.* **2016**, *72*, 2–31. [[CrossRef](#)]
30. Ma, Y.; Chen, Y.; Zhang, F. Power battery life prediction method based on extended H_∞ particle filter algorithm. *Chin. J. Mech. Eng.* **2019**, *55*, 36–43.
31. Zhang, H.; Miao, Q.; Zhang, X. An improved unscented particle filter approach for lithium-ion battery remaining useful life prediction. *Microelectron. Reliab.* **2018**, *81*, 288–298. [[CrossRef](#)]
32. Wei, H.; An, J.; Cheng, J. Realization of RUL prediction of lithium-ion battery based on improved particle filter algorithm. *Automot. Eng.* **2019**, *41*, 1377–1383.
33. Wang, R.; Feng, H. Lithium-ion batteries remaining useful life prediction using Wiener process and unscented particle filter. *J. Power Electron.* **2020**, *20*, 270–278. [[CrossRef](#)]
34. Cheng, W.; Cai, Y.; Su, Y. Remaining life prediction of lithium-ion battery based on improved particle filter. *China Test* **2021**, *47*, 148–153.
35. Tai, Y.; Li, P.; Zheng, Y. Entropy Generation and Thermoelastic Damping in the In-plane Vibration of Microring Resonators. *Entropy* **2019**, *21*, 631. [[CrossRef](#)] [[PubMed](#)]
36. Gu, Q. Research on Li-ion Battery State of Health Estimation Based on Multi-feature Variable Extraction. Master's Thesis, Kunming University of Science and Technology, Kunming, China, 2021.
37. Choi, W.; Shin, H.-C.; Kim, J.M. Modeling and Applications of Electrochemical Impedance Spectroscopy (EIS) for Lithium-ion Batteries. *J. Electrochem. Sci. Technol.* **2020**, *11*, 786–812. [[CrossRef](#)]
38. Yao, L.; Xu, S.; Tang, A.; Zhou, F.; Hou, J.; Xiao, Y.; Fu, Z. Prediction of remaining life of lithium-ion battery based on charge transfer resistance. *Chin. J. Mech. Eng.* **2021**, *57*, 105–117.
39. Tian, Y.; Zeng, G.; Rutt, A.; Shi, T.; Kim, H.; Wang, J.; Ceder, G. Estimation of charge transfer resistance of lithium-ion batteries at different temperatures and states of charge. *Automot. Eng.* **2020**, *42*, 445–453.
40. Mingant, R.; Bernard, J.; Sauvant-Moynot, V. Novel state-of-health diagnostic method for Li-ion battery in service. *Appl. Energy* **2016**, *183*, 390–398. [[CrossRef](#)]
41. Saha, B.; Goebel, K.; Christophersen, J. Comparison of prognostic algorithms for estimating remaining useful life of batteries. *Trans. Inst. Meas. Control* **2009**, *31*, 293–308. [[CrossRef](#)]
42. Ma, Z.; Chen, Y.; Wu, J. Ecological optimization for a combined diesel-organic Rankine cycle. *AIP Adv.* **2019**, *9*, 015320. [[CrossRef](#)]
43. Wang, X.; Wei, X.; Dai, H. Estimation of state of health of lithium-ion batteries based on charge transfer resistance considering different temperature and state of charge. *J. Energy Storage* **2019**, *21*, 618–631. [[CrossRef](#)]
44. Zhou, Y.; Huang, M.; Chen, Y.; Tao, Y. A novel health indicator for on—line lithium—ion batteries remaining useful life prediction. *J. Power Sources* **2016**, *321*, 1–10. [[CrossRef](#)]
45. He, Z.; Wei, T.; Pan, C.; Zhou, H.; Li, Y. An indirect prediction method of lithium-ion battery remaining life based on particle filter and polynomial regression. *J. Chongqing Univ. Technol.* **2020**, *34*, 27–33.
46. Wang, R.; Feng, H. Remaining useful life prediction of lithium-ion battery using a novel health indicator. *Qual. Reliab. Eng. Int.* **2021**, *37*, 1232–1243. [[CrossRef](#)]
47. Xiao, G.; Zhang, H.; Sun, N. Cooperative link scheduling for RSU-assisted dissemination of basic safety messages. *Wirel. Netw.* **2021**, *27*, 1335–1351. [[CrossRef](#)]
48. Zhao, Q.; Cai, Y.; Wang, X. Prediction of the remaining service life of lithium-ion batteries in their entire life cycle. *J/OJ. Power Supply* **2021**, *2095*, 1–14.
49. Liu, D.; Zhou, J.; Liao, H. A Health Indicator Extraction and Optimization Framework for Lithium-Ion Battery Degradation Modeling and Prognostics. *IEEE Trans. Syst. Man Cybern. Syst.* **2015**, *45*, 915–928.
50. Wang, F.-K.; Mamo, T. A hybrid model based on support vector regression and differential evolution for remaining useful lifetime prediction of lithium-ion batteries. *J. Power Sources* **2018**, *401*, 49–54. [[CrossRef](#)]
51. Su, C.; Chen, H.; Wen, Z. Prediction of remaining useful life for lithium-ion battery with multiple health indicators. *Eksploatacja I Niezawodnosc-Maint. Reliab.* **2021**, *23*, 176–183. [[CrossRef](#)]
52. Liang, D.; Gao, J.; Xi, J. RUL prediction of power battery based on multi-feature fusion. *China Test* **2021**, *47*, 149–156.
53. Chen, L.; Zhang, Y.; Zheng, Y. Remaining useful life prediction of lithium-ion battery with optimal input sequence selection and error compensation. *Neurocomputing* **2020**, *414*, 245–254. [[CrossRef](#)]
54. Cheng, Z.; Lu, Z. Research on Load Disturbance Based Variable Speed PID Control and a Novel Denoising Method Based Effect Evaluation of HST for Agricultural Machinery. *Agriculture* **2021**, *11*, 960. [[CrossRef](#)]
55. Tian, J.; Wang, Q.; Ding, J. Integrated Control With DYC and DSS for 4WID Electric Vehicles. *IEEE Access* **2019**, *7*, 124077–124086. [[CrossRef](#)]
56. Sun, Y.; Hao, X.; Pecht, M.; Zhou, Y. Remaining useful life prediction for lithium-ion batteries based on an integrated health indicator. *Microelectron. Reliab.* **2018**, *88*, 1189–1194. [[CrossRef](#)]
57. Wu, J.; Zhang, C.; Chen, Z. An online method for lithium-ion battery remaining useful life estimation using importance sampling and neural networks. *Appl. Energy* **2016**, *173*, 134–140. [[CrossRef](#)]
58. Zhang, J.; Wang, P.; Chen, Z. Joint estimation of SOC-SOH-RUL for lithium-ion batteries based on charging voltage segment and fusion method. *Power Grid Technol.* **2022**, *46*, 1063–1072.

59. Chen, W.; Cai, Y.; Su, Y. Research on Indirect Prediction Method of Remaining Life of Li-ion Battery. *Power Technol.* **2021**, *45*, 719–722.
60. Xu, X.; Lin, P. Parameter identification of sound absorption model of porous materials based on modified particle swarm optimization algorithm. *PLoS ONE* **2021**, *16*, e0250950. [[CrossRef](#)]
61. Li, Y.; Ma, Z.; Zheng, M. Performance Analysis and Optimization of a High-Temperature PEMFC Vehicle Based on Particle Swarm Optimization Algorithm. *Membranes* **2021**, *11*, 691. [[CrossRef](#)]
62. Yang, D.; Zhang, X.; Pan, R. A novel Gaussian process regression model for state-of-health estimation of lithium-ion battery using charging curve. *J. Power Sources* **2018**, *384*, 387–395. [[CrossRef](#)]
63. Wu, J.; Wang, Y.; Zhang, X. A novel state of health estimation method of Li-ion battery using group method of data handling. *J. Power Sources* **2016**, *327*, 457–464. [[CrossRef](#)]
64. Agudelo, B.O.; Zamboni, W.; Monmasson, E. Application domain extension of incremental capacity-based battery SoH indicators. *Energy* **2021**, *234*, 121224. [[CrossRef](#)]
65. Guo, P.; Zhang, C.; Gao, X. State-of-health estimation method for ternary lithium-ion battery based on capacity increment curve. *Glob. Energy Internet* **2018**, *1*, 180–187.
66. Fly, A.; Chen, R. Rate dependency of incremental capacity analysis (dQ/dV) as a diagnostic tool for lithium—ion batteries. *J. Energy Storage* **2020**, *29*, 101329. [[CrossRef](#)]
67. Pan, W.; Luo, X.; Zhu, M. A health indicator extraction and optimization for capacity estimation of Li-ion battery using incremental capacity curves. *J. Energy Storage* **2021**, *42*, 469–502. [[CrossRef](#)]
68. Li, H. Capacity Estimation and Consistency Screening of Decommissioned Batteries Based on IC Curves. Master's Thesis, Dalian University of Technology, Dalian, China, 2021.
69. Yang, S.; Luo, B.; Wang, J. Estimation of Lithium-ion Battery State of Health Based on Characteristic Parameters of Capacity Increment Curve Peak Interval. *Chin. J. Electrotech. Technol.* **2021**, *36*, 2277–2287.
70. Li, Y.; Abdel-Monem, M.; Gopalakrishnan, R. A quick on-line state of health estimation method for Li-ion battery with incremental capacity curves processed by Gaussian filter. *J. Power Sources* **2018**, *373*, 40–53. [[CrossRef](#)]
71. Tang, X.; Zou, C.; Yao, K. A fast estimation algorithm for lithium-ion battery state of health. *J. Power Sources* **2018**, *396*, 453–458. [[CrossRef](#)]
72. Pang, X.; Liu, X.; Jia, J. A lithium-ion battery remaining useful life prediction method based on the incremental capacity analysis and Gaussian process regression. *Microelectron. Reliab.* **2021**, *127*, 114405. [[CrossRef](#)]
73. Feng, H.; Zhang, X. Estimation of State of Health and Remaining Life Prediction of Lithium Batteries Based on New Health Factors. *J. Nanjing Univ.* **2021**, *57*, 660–670.
74. Zhu, R. Research on the Remaining Life of Lithium Batteries with Multi-Indicator Fusion under the Charging Curve. Master's Thesis, Beijing Jiaotong University, Beijing, China, 2020.
75. Gao, Y.; Jiang, J.; Zhang, C.; Zhang, W.; Jiang, Y. Aging mechanisms under different state-of-charge ranges and the multi-indicators system of state-of-health for lithium-ion battery with Li(NiMnCo)O₂ cathode. *J. Power Sources* **2018**, *400*, 641–651. [[CrossRef](#)]
76. Feng, H.; Song, D. A health indicator extraction based on surface temperature for lithium-ion batteries remaining useful life prediction. *J. Energy Storage* **2021**, *34*, 102118. [[CrossRef](#)]
77. Afshari, S.S.; Cui, S.; Xu, X. Remaining Useful Life Early Prediction of Batteries Based on the Differential Voltage and Differential Capacity Curves. *IEEE Trans. Instrum. Meas.* **2022**, *71*, 3117631. [[CrossRef](#)]
78. Cheng, Z.; Zhou, H.; Lu, Z. A Novel 10-Parameter Motor Efficiency Model Based on I-SA and Its Comparative Application of Energy Utilization Efficiency in Different Driving Modes for Electric Tractor. *Agriculture* **2022**, *12*, 362. [[CrossRef](#)]
79. Li, X.; Deng, T.; Wang, M. Improvement of Linear Location Algorithm of Wood Acoustic Emission Source Based on Wavelet and Correlation Analysis. *Chin. J. For. Eng.* **2020**, *5*, 138–143. [[CrossRef](#)]
80. Zhang, Y.; Xiong, R.; He, H. Lithium-Ion Battery Remaining Useful Life Prediction With Box-Cox Transformation and Monte Carlo Simulation. *IEEE Trans. Ind. Electron.* **2019**, *66*, 1585–1597. [[CrossRef](#)]
81. Shu, X.; Liu, Y.; Shen, J. Prediction of Li-ion Battery Capacity Based on Improved Least Squares Support Vector Machine and Box-Cox Transform. *Chin. J. Mech. Eng.* **2021**, *57*, 118–128.
82. Bingchen, H.; Xueming, Y.; Jinsong, W.; Xu, Z.; Zongjie, H.; Qiang, L. Remaining service life prediction of lithium-ion battery based on PCA-GPR. *J. Sol. Energy* **2022**, *43*, 484–491. [[CrossRef](#)]
83. Pang, X.Q.; Wang, Z.Q.; Zeng, J.C.; Jia, J.F.; Shi, Y.H.; Wen, J. Prediction of Remaining Service Life of Li-ion Batteries Based on PCA-NARX. *J. Beijing Inst. Technol.* **2019**, *39*, 406–412. [[CrossRef](#)]
84. Shi, Y.; Shi, M.; Ding, E. Remaining life prediction of lithium-ion battery based on multiple degradation characteristics. *Power Technol.* **2020**, *44*, 836–840.
85. Wang, Z.; Pang, X.; Huang, R. RUL prediction of lithium-ion battery based on KPCA-ANFIS. *J. Electron. Meas. Instrum.* **2018**, *32*, 26–32.
86. Liu, J.; Chen, Z. Remaining Useful Life Prediction of Lithium-Ion Batteries Based on Health Indicator and Gaussian Process Regression Model. *IEEE Access* **2019**, *7*, 39474–39484. [[CrossRef](#)]
87. Venugopal, P.; Shankar, S.S.; Jebakumar, C.P. Analysis of Optimal Machine Learning Approach for Battery Life Estimation of Li-Ion Cell. *IEEE Access* **2021**, *9*, 159616–159626. [[CrossRef](#)]